Remote Sensing Retrieval of Isoprene Concentrations in the Southern Ocean

Pablo Rodríguez-Ros, Martí Galí, Pau Cortés, Charlotte Mary Robinson, David Antoine, Charel Wohl, Mingxi Yang, Rafel Simó

Geophysical Research Letters

RESEARCH LETTER
10.1029/2020GL087888

Remote Sensing Retrieval of Isoprene Concentrations in the Southern Ocean

Pablo Rodríguez-Ros[1], Martí Galí[2], Pau Cortés[1], Charlotte Mary Robinson[3], David Antoine[3,4], Charel Wohl[5], MingXi Yang[5], and Rafel Simó[1]

[1]Institut de Ciències del Mar, ICM-CSIC, Passeig Marítim de la Barceloneta, Barcelona, Catalonia, Spain, [2]Earth Sciences Department, Barcelona Supercomputing Center (BSC-CNS), Barcelona, Catalonia, Spain, [3]Remote Sensing and Satellite Research Group, School of Earth and Planetary Sciences, Curtin University, Perth, Western Australia, Australia, [4]Sorbonne Université, CNRS, Laboratoire d'Océanographie de Villefranche, LOV, Villefranche-sur-Mer, France, [5]Plymouth Marine Laboratory, Plymouth, UK

Key Points:
- We present an algorithm for the retrieval of isoprene concentrations in the Southern Ocean from remote sensing
- Isoprene peaks in midsummer and is highest in coastal and near-island waters and in the 40–50°S latitudinal band
- The annual isoprene emission from the entire Southern Ocean amounts 63 Gg C yr^{-1}

Supporting Information:
- Supporting Information S1
- Figure S1
- Figure S2
- Figure S3
- Figure S4
- Figure S5

Correspondence to:
R. Simo,
rsimo@icm.csic.es

Citation:
Rodríguez-Ros, P., Galí, M., Cortés, P., Robinson, C. M., Antoine, D., Wohl, C., et al. (2020). Remote sensing retrieval of isoprene concentrations in the Southern Ocean. *Geophysical Research Letters*, *47*, e2020GL087888. https://doi.org/10.1029/2020GL087888

Received 11 MAR 2020
Accepted 29 MAY 2020
Accepted article online 4 JUN 2020

Abstract Isoprene produced by marine phytoplankton acts as a precursor of secondary organic aerosol and thereby affects cloud formation and brightness over the remote oceans. Yet the marine isoprene emission is poorly constrained, with discrepancies among estimates that reach 2 orders of magnitude. Here we present ISOREMS, the first satellite-only based algorithm for the retrieval of isoprene concentration in the Southern Ocean. Sea surface concentrations from six cruises were matched with remotely sensed variables from MODIS Aqua, and isoprene was best predicted by multiple linear regression with chlorophyll a and sea surface temperature. Climatological (2002–2018) isoprene distributions computed with ISOREMS revealed high concentrations in coastal and near-island waters, and within the 40–50°S latitudinal band. Isoprene seasonality paralleled phytoplankton productivity, with annual maxima in summer. The annual Southern Ocean emission of isoprene was estimated at 63 Gg C yr^{-1}. The algorithm can provide spatially and temporally realistic inputs to atmospheric and climate models.

Plain Language Summary Isoprene is a marine trace gas with climatic relevance in remote regions of the ocean, because it reacts readily in the atmosphere to produce aerosols (atmospheric particles) that make clouds brighter. In the Southern Ocean, however, its regional emission is poorly quantified. We explored the capability of satellite observations (MODIS Aqua, NASA) to reconstruct isoprene concentrations measured in the Southern Ocean during various oceanographic cruises. We found an empirical relationship between isoprene and sea surface chlorophyll and temperature and used it to produce regional maps of isoprene emission. The new tool presented here, named ISOREMS, enables detailed exploration of the role of ocean-leaving isoprene in the Southern Ocean atmosphere.

1. Introduction

Marine aerosols control cloud microphysics and optics over the oceans (Andreae & Rosenfeld, 2008). Trace gases of marine origin, when oxidized in the lower atmosphere, form new aerosol particles and condense on preexisting ones. These particles can eventually grow large enough to act as cloud condensation nuclei (CCN), increasing cloud brightness and lifetime (Carslaw et al., 2013). When the particle-forming oxidation products are mainly organic, the resulting aerosols are named secondary organic aerosols (SOA) (O'Dowd et al., 2004). Ocean-emitted isoprene (2-methyl-1,3-butadiene, C_5H_8) contributes between 5% and 25% of the natural SOA sources in the global marine atmosphere (Claeys et al., 2004; Gantt et al., 2009; Luo & Yu, 2010; Liao et al., 2007). Owing to its high reactivity (1–2 hr lifetime) (Medeiros et al., 2018), isoprene can impact the chemistry of the marine boundary layer (Lewis et al., 2005; Palmer & Shaw, 2005) and cool the climate (Carslaw et al., 2013: Claeys et al., 2004). This impact is thought to be stronger in the Southern Ocean (SO), away from land vegetation emissions, where isoprene can act synergistically with marine dimethylsulfide to form CCN (Booge et al., 2016; Dani & Loreto, 2017; Meskhidze & Nenes, 2006; Vallina et al., 2007).

Although it has been suggested that depending on the regional magnitude of its emission fluxes, marine isoprene should be taken into account in climate models (Gantt et al., 2009; Shaw et al., 2010), this objective is currently hampered by the lack of knowledge about its drivers, spatiotemporal distribution, and atmospheric

effects (Carslaw et al., 2013). Even the magnitude of marine isoprene emission is largely unconstrained, and there still are large discrepancies between the bottom-up (0.085–1.2 Tg C yr^{-1}; Arnold et al., 2009; Bonsang et al., 1992; Booge et al., 2016; Broadgate et al., 1997; Gantt et al., 2009; Milne et al., 1995; Palmer & Shaw, 2005) and the top-down (1.9–11.6 Tg C yr^{-1}Arnold et al., 2009; Luo & Yu, 2010) estimates of the global oceanic flux. Most of the discrepancy stems from limited knowledge of isoprene production and loss processes in sea water (Booge et al., 2016, 2018; Brüggemann et al., 2018; Shaw et al., 2010), and the relationship between isoprene concentrations and biological and environmental parameters (Carpenter et al., 2012; Exton et al., 2013).

Due to the scarcity of in situ data, large-scale estimates of isoprene must rely on either process-based ecosystem models or empirical models based on remote sensing data. Process-based isoprene parameterizations are currently limited by poor knowledge of the underlying processes. Therefore, empirical models linking directly observed sea surface concentrations and remotely sensed variables offer a workable alternative for mapping isoprene, while allowing for uncertainty estimates. According to the available observations, higher marine isoprene concentrations tend to cooccur with phytoplankton blooms (Ooki et al., 2015). In the SO, local foci of iron supply lead to higher productivity and are expected to result in higher isoprene, as confirmed by deliberate iron fertilization experiments (Wingenter et al., 2004). The close relationship of isoprene to primary production and phytoplankton biomass, further tuned by environmental drivers such as temperature and light, has been demonstrated by both laboratory experiments and measurements at sea (Bonsang et al., 2010; Exton et al., 2013; Liakakou et al., 2007; McKay et al., 1996; Meskhidze et al., 2015; Milne et al., 1995; Moore et al., 1994; Shaw et al., 2003). Therefore, chlorophyll a (CHL) concentration has been proposed, either alone or together with temperature or light, to empirically estimate isoprene concentration and emission from remote sensing observations (Bonsang et al., 1992; Booge et al., 2016; Hackenberg et al., 2017; Ooki et al., 2015). In their pioneering work, Palmer and Shaw (2005) used a mixed approach that combined MODIS (Moderate-resolution Imaging Spectroradiometer) CHL observations with a steady state water column model, parameterizing isoprene production from experimentally determined chlorophyll a-specific production rates and prescribing microbial and chemical losses at fixed rate constants. Arnold et al. (2009), Luo and Yu (2010), and Booge et al. (2016) went a step further by using remote sensing estimates of phytoplankton functional types (PFT) and applying PFT-specific production rates from phytoplankton culture experiments.

The aforementioned models suggested that high southern latitudes are strong emitters of marine isoprene, by concurrence of high seasonal productivity and strong winds. Therefore, several circumstances concur in the SO that warrant a focused effort to assess isoprene emissions from remote sensing: potential for high emissions due to productivity and wind speed, cleanliness of the atmosphere, and remoteness from continental influence. However, there has been a paucity of measurements of isoprene concentrations in the region (Hackenberg et al., 2017; Kameyama et al., 2014; Ooki et al., 2015). In the present work, we utilize an unprecedented data set of isoprene concentrations from six research voyages (two of them reported here for the first time), which collectively span a much larger area than ever observed in situ, to develop an algorithm for the retrieval of isoprene from remote sensing in the SO. The algorithm, here used to generate monthly synoptic distributions of isoprene concentration and emission fluxes, should allow the evaluation of interannual variability and decadal trends, and can be used to feed atmospheric models to assess ocean-climate interactions in this sensitive and critical region of the Earth.

2. In Situ Measurements

The PEGASO cruise was conducted in January 2015 on board the RV *Hesperides* in waters of the Atlantic sector of the SO, the Antarctic Peninsula, and the Weddell Sea (Nunes et al., 2019; Rodrguez-Ros et al., 2020; Zamanillo et al., 2019). The ACE cruise circumnavigated the SO between December 2016 and April 2017 on board the RV *Akademik Tryoshnikov* (Rodrguez-Ros et al., 2020). During both cruises, seawater samples were collected from either the underway pumping system (intake at ≈4–5 m depth) or the uppermost (≈5 m) bottle of the rosette on CTD casts. In either case, 0.5 L all-glass bottles were completely filled leaving no headspace, and analyzed within 1 hr after collection. Isoprene was measured, along with other volatile compounds, on a gas chromatography-mass spectrometry system (5975-T LTM-GC/MSL, Agilent Technologies). Aliquots of 25 ml were taken from the glass bottle with a glass syringe with a teflon tube

and filtered through a GF/F filter while introduced into a purge and trap system (Stratum, Tekmar Teledyne). Volatiles were stripped by bubbling with 40 ml min^{-1} of ultrapure He for 12 min, trapped on solid adsorbent at room temperature and thermally desorbed (250°C) into the GC. Isoprene, monitored as m/z 67 in selected ion monitoring mode, had a retention time of 2.4 min in the LTM DB-VRX chromatographic column held at 35°C. The detection limit was 1 pmol L^{-1}. All samples were run in duplicates. In PEGASO, calibration was performed by injections of a gaseous mixture of isoprene in N_2. In ACE, a liquid standard solution prepared in cold methanol was used instead. In situ chlorophyll concentrations (CHL_{fluo}) were determined by filtration of 250 ml (PEGASO) or 2,000 ml (ACE) of sea water through GF/F filters, extraction with cold 90% acetone for 24 hr, and fluorescence measurement of extracts on a calibrated Turner Designs fluorometer.

For model development and validation, we also compiled surface (0–10 m depth) isoprene, CHL and temperature data from four other research cruises conducted entirely or partly in the SO (>40°S), namely: KH-09-5-2010 (Ooki et al., 2015), AMT23-2013 and AMT22-2012 (Hackenberg et al., 2017), and ANDREXII-2019 (Wohl et al., 2020) (Table S1 in the supporting information and Figure 1). Description of measurement procedures can be found in the corresponding publications. Another cruise was discarded for this analysis because the reported isoprene concentrations were much higher than any other cruise's in the region (Kameyama et al., 2014), and there is the suspicion that they had a systematic offset (S. Kameyama, personal communication, April 2019). A frequency distribution analysis reveals that isoprene measurements of the entire data set were evenly spread across the diel solar cycle (Figure S1), probably because a large proportion of the database is contributed by automated instruments or underway measurements at high temporal resolution (ANDREXII, KH-09-5, part of PEGASO).

3. Remote Sensing Matchups

We matched the in situ measurements (Table S1) with several remotely sensed variables including CHL, sea surface temperature (SST), photosynthetically available radiation (PAR), euphotic layer depth (ZEU), particulate inorganic carbon (PIC), and particulate organic carbon (POC). MODIS-Aqua daily, 8-day and monthly composites at 4.64-km resolution were obtained from the NASA Ocean Color Website, accessed in February 2020, MODIS-AOCL (2019), https://oceancolor.gsfc.nasa.gov/) (Table S2). The SO is challenging for remote sensing of ocean color due to persistent heavy clouds, presence of sea ice, and low Sun angles (Neukermans et al., 2018). To overcome the frequent satellite data gaps, match-ups were searched sequentially in order of decreasing spatial-temporal resolution until a valid value was found. For the time and position of each in situ measurement, the search started with the daily single-pixel value, continued with the average of 3×3 and 5×5 pixel bins centered around it, and proceeded similarly for 8-day and monthly composites, ensuring that the best available resolution was used (Galí et al., 2018). Finally, in situ measurements that corresponded to the same satellite datum were averaged to avoid overrepresentation. The resulting database of isoprene and satellite measurements was matched to the mixed layer depth (MLD) obtained from a global monthly $1° \times 1°$ climatology (Holte et al., 2017).

4. ISOREMS: A New Remote Sensing-Based Model to Predict Isoprene Concentrations in the Southern Ocean

We explored the predictive capacity of each remotely sensed variable for isoprene concentration through linear regression analysis. The best paired relationship was with CHL ($r^2 = 0.15$, p value <0.05, $n = 408$), followed by SST ($r^2 = 0.09$, p value <0.05, $n = 408$). A redundancy analysis (Legendre & Legendre, 2012) revealed that both CHL and SST contributed to the variance of isoprene concentration, while other variables were highly redundant to either CHL (POC, ZEU) or SST (PAR) (Figure S2). The fit improved indeed with a multiple regression model with CHL and SST together ($r^2 = 0.24$, p value <0.05). To further improve the model, we excluded three subsets that degraded the fit disproportionately, such that a total of 327 points were retained out of 408 (80%). Two of the subsets were removed owing to large discrepancies between in situ and satellite CHL, whose uncertainty propagated to the regression model. This was the case with some samples from the bloom north of South Georgia Islands, where diatoms represented more than 80% of the phytoplankton community (Nunes et al., 2019); under these particular conditions, standard algorithms for CHL determination from satellite show poor agreement to in situ CHL_{fluo} due to the interference of

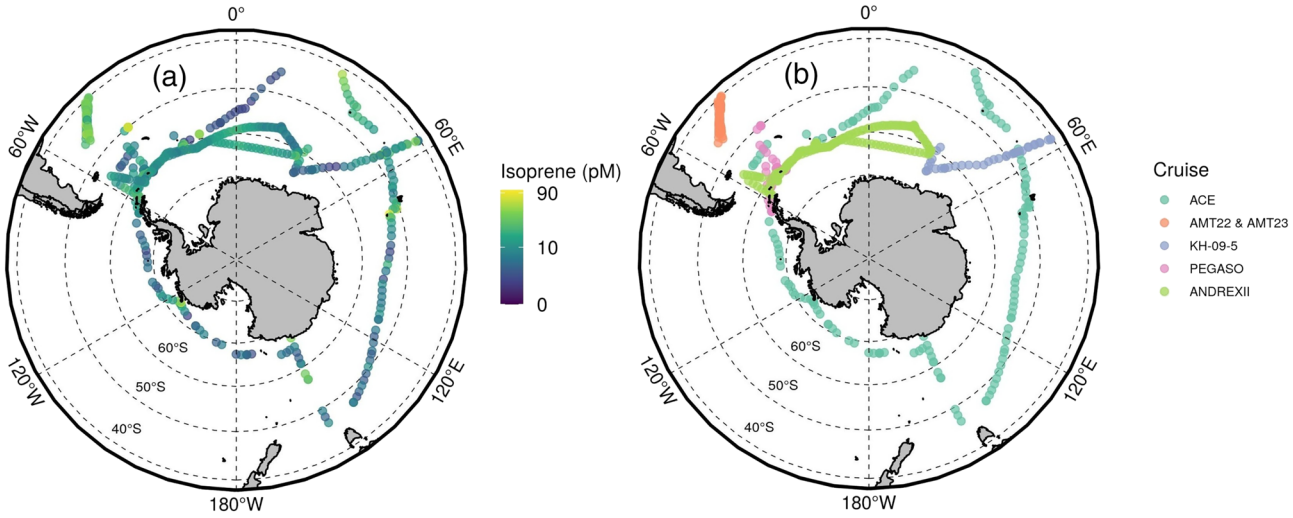

Figure 1. (a) Surface ocean isoprene concentrations from the six cruises. Note the log scale. (b) Cruise tracks. More information is listed in Table S1 in the supporting information.

chlorophyll c pigments (Moutier et al., 2019). We also excluded from the database the cases where CHL values fell out of the 90% confidence prediction intervals of the regression between CHL and their CHL_{fluo} match-ups ($r^2 = 0.63$, p value <0.05); this criterion removed points where the discrepancy could have been due either to optical reasons (which could not be assessed in the original data sets), or to poor match-up (e.g., due to strong small-scale variability). Finally, we also excluded two cases with CHL higher than 2 μg L^{-1} that were flagged outliers in the isoprene versus CHL regression. The resulting multiple regression model between isoprene and CHL + SST improved after these removals (Equation 1, $r^2 = 0.45$, MAPE = 46%, RMSE = 10.6 pM, relative RMSE = 0.73, relative BIAS = −0.5%, $n = 327$), and we named it ISOREMS (*Isoprene Southern Ocean Remote Sensing*) (numbers in brackets show the 95% confidence interval for each coefficient, estimated as described in section 5):

$$\mathrm{ISO} = 3.0\ [1.9 - 4.2] + 35.22\ [29.35 - 40.08] \cdot \mathrm{CHL} + 0.68\ [0.59 - 0.77] \cdot \mathrm{SST} \quad (1)$$

where ISO is predicted isoprene concentration in pM (pmol L^{-1}), CHL is satellite-derived chlorophyll a concentration, and SST is satellite-derived sea surface temperature in degrees celsius (°C). We note that ISOREMS is developed from observations within the following ranges: 0.04–1.54 μg L^{-1} CHL, −1.8–24.5°C SST, 72.42S–40.00S latitude, and its applicability is uncertain beyond these ranges. However, note that the proportion of 1 × 1° pixels with climatological CHL >1.54 μg L^{-1} is only 1.8% in October through March and 0.7% during the rest of the year. In Figure 2, we display the scatter plot of the predicted versus observed isoprene concentrations. In Figure S3 the residuals of ISOREMS predictions are shown to explore the misfit with observations along ranges of the potential predictor variables (CHL, SST, PAR, ZEU, PIC, POC, and MLD). The misfit between predictions and observations is typically in the range of −30 to +30 pM, with the largest differences corresponding to six measurements from the diatom bloom in PEGASO (Nunes et al., 2019; Zamanillo et al., 2019). The analysis of the residuals (Figure S3) does not support the addition of any of the other potential predictors or the need for nonlinear terms in the multiple regression.

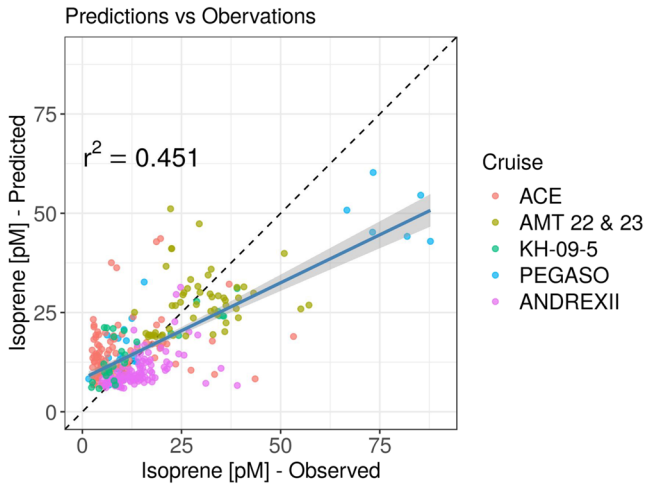

Figure 2. Scatter plot of ISOREMS predictions versus observations of isoprene concentrations.

5. Validation of ISOREMS

Since all available data in the SO were used to develop ISOREMS, a random sampling approach was taken to validate the performance of the

algorithm. First, a multiple regression model equivalent to ISOREMS was performed on 80% of in situ isoprene and matched satellite CHL and SST data set. The resulting equation was then applied to the remaining 20% of the data set, and predicted values were compared to observations using an array of skill metrics. We ran a total of 10,000 simulations following this process, which provided us with robust estimates of ISOREMS coefficients and skill metrics, along with their respective confidence intervals. Scatter plots of the randomly generated ISOREMS coefficients (Figure S4a) indicate a negative relationship between the intercept and the CHL coefficient in Equation 1, contrasting with the independent behavior of the SST coefficient. This exercise reveals a trade-off in the ability of ISOREMS to fit low isoprene concentrations (more influenced by the intercept) or high concentrations (more influenced by the CHL coefficient). Moreover, it suggests that additional predictor variables may be needed to obtain better fits. Unfortunately, inclusion of none of the other tested variables (Table S2) improved ISOREMS significantly. Finally, the histograms of the 10,000 randomly generated ISOREMS validation statistics (Figure S4b) are clearly centered around the statistics obtained when fitting the entire data set (Table S1). Therefore, these statistics can reliably be used as uncertainty estimates of ISOREMS predictions on a pixel basis.

6. ISOREMS Implementation to Compute Isoprene Concentrations and Emission Fluxes

We implemented the ISOREMS model using monthly climatological fields of CHL and SST from MODIS-Aqua for the period 2002–2018 from NASA Ocean Color service (https://oceancolor.gsfc.nasa.gov/). We then used the resulting concentrations of $ISO_{ISOREMS}$ to calculate the air-sea flux of isoprene (Palmer & Shaw, 2005):

$$F_{ISO} = k_{AS} \cdot \left(ISO_w - \frac{ISO_a}{K_H} \right) \approx k_{AS} \cdot ISO_w \tag{2}$$

Where ISO_w is isoprene concentration in sea water, ISO_a is isoprene concentration in the air, K_H is the Henry's Law constant for isoprene, and k_{AS} is the gas exchange velocity (cmh^{-1}). Air-side isoprene can be considered near zero and neglected for flux calculations because (a) isoprene is typically largely supersaturated in the surface ocean (>700% during ANDREXII Wohl et al., 2020), and (b) its short atmospheric lifetime (Medeiros et al., 2018) prevents that high airborne isoprene concentrations of continental origin occurred during our sampling. For k_{AS} we used the Wanninkhof (2014) parameterization:

$$k_{AS} = 0.251 \cdot <U_{10}^2> \cdot \left(\frac{S_C}{660} \right)^{-0.5} \tag{3}$$

Where $<U_{10}^2>$ is the average of the square of the wind speed at 10 m ($m^2\ s^{-2}$), and Sc is the *Schmidt* number (nondimensional). We used monthly mean climatological fields of U_{10}^2 at 1 × 1° spatial resolution constructed from the CCMPv2 product at 0.25 × 0.25° and 6-hr resolution for the period 1987–2018, which includes data from many intercalibrated satellites (all the information and the most recent estimates are available at https://www.remss.com/measurements/wind/). To calculate Sc we used the equation proposed by Palmer and Shaw (2005):

$$S_C = 3913.15 - 162.13 \cdot SST + 2.67 \cdot SST^2 - 0.012 \cdot SST^3 \tag{4}$$

Where SST is in degrees celsius (°C).

7. ISOREMS-Derived Isoprene Concentrations and Emission in the Southern Ocean

Our climatological monthly concentrations and air-sea fluxes of isoprene in the SO show remarkable coupling to biological productivity, with higher values in coastal regions, such as the Antarctic and South Atlantic Shelves, and next to subantarctic islands (Figures 3 and S5). This is expected from Equation 1and consistent with previous fieldwork studies (Broadgate et al., 2004; Hackenberg et al., 2017; Ooki et al., 2015; Zindler et al., 2014).

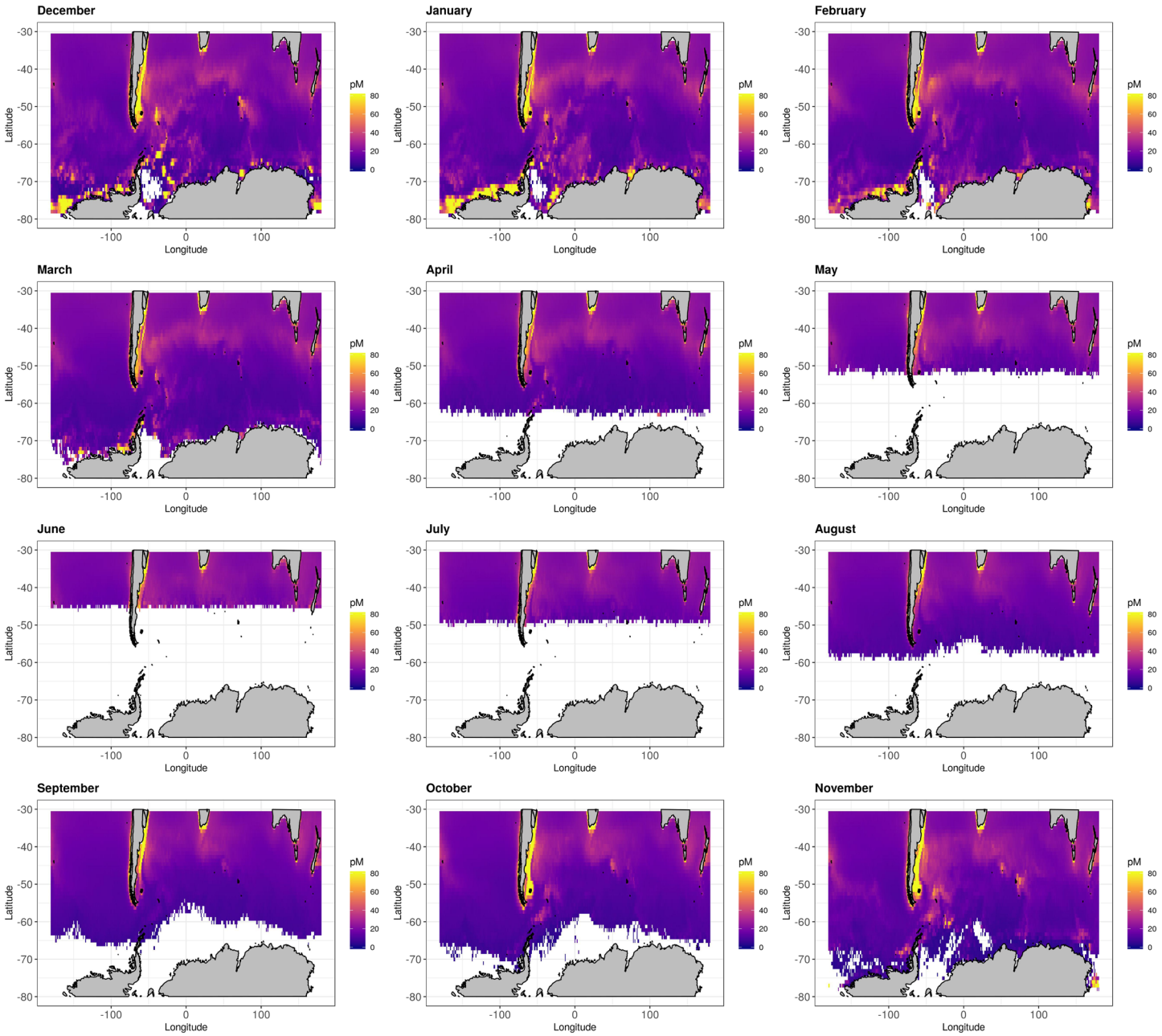

Figure 3. Monthly climatology of $ISO_{ISOREMS}$ concentration in the Southern Ocean.

A band of higher isoprene concentrations and air sea fluxes is observed around the Subantarctic front (approximately between 40°S and 50°S), as already depicted by Ooki et al. (2015) and Wohl et al. (2020). However, the air sea fluxes show a more spread distribution than concentrations, with weaker gradients toward continental shelves and islands. This is consistent with the modeling simulations of Luo and Yu (2010) and Booge et al. (2016). Monthly average concentrations of $ISO_{ISOREMS}$ in the entire SO peak in January (13 pM), and the annual mean throughout the climatological year is 7 pM (Figure 4a). By latitudes, concentrations are higher in the 40–50°S band (Figure 4b), reaching maximum values above 20 pM in November–December (Figure 4a). The 50–60°S and 60–70°S bands also show clear seasonality, yet their annual maxima are around 16 pM in December and 15 pM in January, respectively (Figure 4a).

As depicted by Figure 3, large portions of the SO are devoid of CHL data over the months of May through August. Consequently, isoprene concentrations cannot be computed in these areas. Similarly, large areas

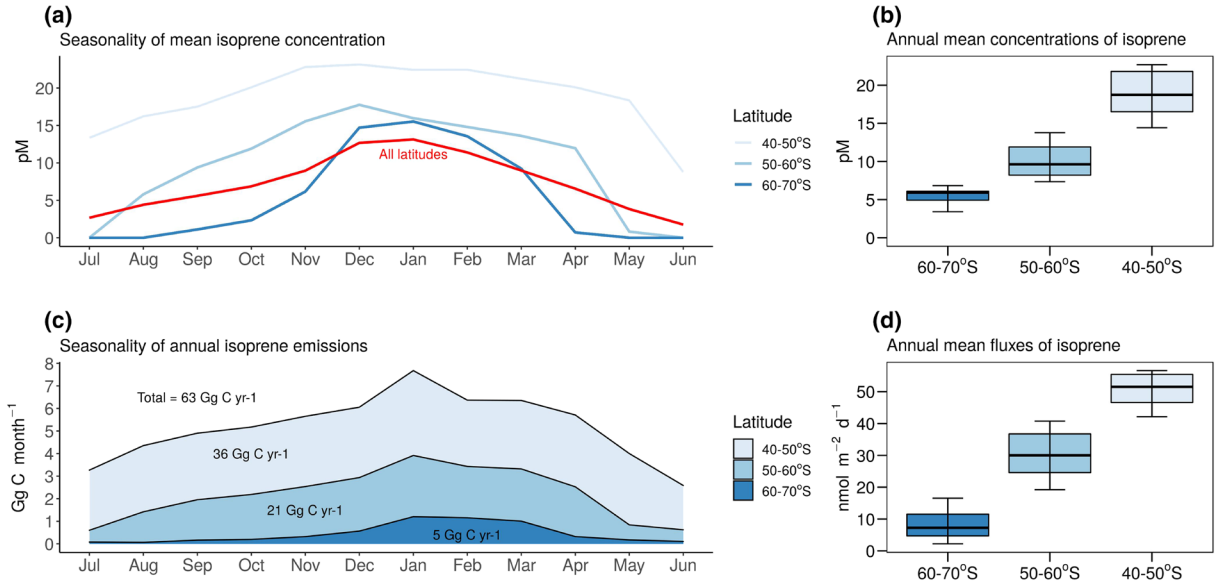

Figure 4. (a) Climatological seasonality of $ISO_{ISOREMS}$ concentrations in the entire Southern Ocean (red) and averaged by latitudinal bands (40 to 70°S). (b) Boxplot of annual mean concentrations of isoprene grouped by latitude. (c) Climatological accumulated emissions of $ISO_{ISOREMS}$ through the year. (d) Boxplot of annual mean isoprene emission fluxes grouped by latitude. In the boxplots (b and d), the horizontal black line inside the boxes is the median, the upper, and lower limits of the boxes are, respectively, 75th and 25th percentiles; and the horizontal bars represent the upper and lower whiskers (largest values within 1.5 times interquartile range above 75th percentile and below 25th percentile).

lack climatological wind speeds in May through August as well as near the Antarctic coasts all year round (Figure S5), impeding calculation of the air sea flux. In order to circumvent this lack of data and be able to estimate SO-integrated isoprene emissions, we made two assumptions: (a) when light is not enough to allow remote sensing of CHL, we assume a minimum isoprene concentration of 3 pM, which is the intercept of Equation 1; (b) the gaps of remote sensing wind speed are filled with a fixed value of 7 m s^{-1}, considered a reasonable approximation to year-round conditions close to the Antarctic coasts (Bintanja et al., 2014). Moreover, following Peng et al. (2013) and Meier et al. (2017) we created a mask of sea ice coverage with monthly averages for 2018, and assumed that isoprene emission is zero at sea ice concentrations above 10% (Galí et al., 2019). Integrating the resulting fluxes, monthly isoprene emissions from the entire SO peak in January (7.9 Gg C $month^{-1}$, Figure 4c), where the highest monthly averaged isoprene fluxes (around 50 nmol m^{-2} day^{-1}) occur in the latitudinal band of 40–50°S (Figure 4d). Integrated over an entire climatological year, isoprene emission in the SO amounts to 63 Gg C yr^{-1}. The latitudinal band of 40–50°S contributes 57% of this emission, and the 50–60°S and 60–70°S bands contribute 33% and 8%, respectively. Note that the SO comprises 27% of the world's ocean area, and our annual isoprene emission (63 Gg C yr^{-1}) represents 5–74% of the bottom-up emission estimates for the global ocean (Arnold et al., 2009; Bonsang et al., 1992; Booge et al., 2016; Broadgate et al., 1997; Gantt et al., 2009; Milne et al., 1995; Palmer & Shaw, 2005), and 0.5–3% of the top-down estimates (Arnold et al., 2009; Luo & Yu, 2010). Therefore, ISOREMS supports the order of magnitude of the bottom-up approaches to marine isoprene emissions.

8. Caveats of ISOREMS and Future Research

8.1. Lack of Observations in a Complex Ocean

The surface waters of the SO are a complex mosaic in terms of biological, environmental, and physical properties (Ardyna et al., 2017). Since Longhurst (1995) described oceanic biogeochemical provinces 35 years ago, there have been several attempts to revisit that concept, reaching different results depending on the criteria used and the purpose of the regionalization (Ardyna et al., 2017; Fay & McKinley, 2014). The conspicuous heterogeneity of the SO makes diagnostic isoprene parameterizations strongly dependent on the distribution of data used to build the statistical model. The paucity of measurements in the SO limited previous attempts

to predict isoprene concentrations from in situ CHL and SST: Ooki et al. (2015) pooled together data from the Arctic and the Antarctic, and Hackenberg et al. (2017) barely explored the northernmost area of the Atlantic sector of the SO (Figure 1, Table S1). We significantly increased the number of isoprene observations and covered most of the biogeochemical provinces, biomes, and bioregions suggested by Fay and McKinley (2014) and Ardyna et al. (2017), yet only in summer or early fall. More observations in heavily undersampled regions like the Pacific sector, and at the beginning and end of the productive season, are needed for a better representation of the spatial and temporal heterogeneity.

8.2. Uncertainties About Potential Sources of Atmospheric Isoprene From the Southern Ocean

In view of the enormous existing discrepancies between top-down and bottom-up approaches to isoprene emissions, a missing oceanic source has been invoked, and interpretation of laboratory experiments has partly attributed it to photoproduction reactions in the surface microlayer (SML), that is, right at the air-sea interface (Ciuraru et al., 2015). Brüggemann et al. (2018) provided a global map of SML isoprene photoproduction factors to calculate the relative contribution of this process to the isoprene production by phytoplankton. Conte et al. (2020) implemented these factors in the PISCES global model and estimated that emissions of isoprene by SML photoproduction represent up to ≈60% of the global emission. Therefore, our ISOREMS emission estimates probably set a lower limit for the total emission of isoprene from the SO, which may increase when a sound parameterization of the SML photoproduction is implemented. However, eddy covariance measurements of the oceanic flux of isoprene over the open ocean at relatively high wind speeds and low light levels have found no evidence for photochemical production of isoprene in the SML (Kim et al., 2017), and isoprene airborne concentrations in the Arctic did not correlate with a proxy of SML photoproduction either (Mungall et al., 2017). It also must be noted that for oceanic regions with persistent high wind speeds, like the SO, the widespread occurrence of an SML is controversial (Brüggemann et al., 2018).

9. Closing Remarks

- ISOREMS is the first published statistical model to predict isoprene concentrations based solely on remote sensing data, which allows synoptic distributions of isoprene concentrations to be computed over the entire SO.
- Similar regional models should be developed for other oceanic regions in order to predict the global patters of isoprene concentration and its emission to the atmosphere. A mosaic of regional models holds better potential than a single model to accurately constrain global isoprene emissions and contribute to close the current existing gap between bottom-up and top-down approaches.
- Our results do not resolve the aforementioned discrepancy but support the order of magnitude of the bottom-up estimates.
- Even though the SO has areas and months of high productivity due to abundance of macronutrients and localized iron supply, isoprene concentrations and emissions are moderated by the low temperatures. This does not preclude they may be important for the SOA budget in a region that is particularly sensitive to aerosols of marine origin.
- ISOREMS represents a useful tool to study the role of oceanic isoprene emissions in climate and the oxidative capacity of the atmosphere over the SO.

Data Availability Statement

Data are available at the *Zenodo* repository (https://doi.org/10.5281/zenodo.3822547, DOI: 10.5281/zenodo.3822547).

Acknowledgments

This research was funded by the Spanish Ministry of Economy and Competitiveness through projects PEGASO (CTM2012-37615) and BIOGAPS (CTM2016-81008-R) to R. S., and partially by the Australian Government through the Australian Research Council's Discovery Projects funding scheme (project DP160103387). The Antarctic Circumnavigation Expedition was made possible by funding from the Swiss Polar Institute and Ferring Pharmaceuticals. P. R. R. was supported by a "la Caixa" Foundation PhD Fellowship (2015–2019). Members of the ACE#1 research team are greatly acknowledged for providing data and technical support. We are grateful to NASA's Ocean Biology Processing Group (OBPG) for MODIS Aqua data and to the British Oceanographic Data Centre (BODC). We thank R. Wanninkhof (NOAA/AOML) and J. Trianes (Universidade de Santiago de Compostela) for providing the CCMP2 monthly climatology. P. R. R. would like to thank M. Babin, M. Levasseur, and M. Lizotte for hosting and training him at Takuvik Joint International Laboratory (Université Laval (Canada) CNRS (France)) during 2016. We also want to thank the Captain, officers, and crew of RV *Hespérides* and RV *Akademik Tryoshnikov*, engineers of the Marine Technology Unit (CSIC), and research colleagues for their support and help during the cruises.

References

accessed in February 2020, M O D I S -A OC L (2019). NASA Goddard Space Flight Center, Ocean Ecology Laboratory, Ocean Biology Processing Group. https://doi.org/10.5067/AQUA/MODIS/L3M/

Andreae, M. O., & Rosenfeld, D. (2008). Aerosol–cloud–precipitation interactions. Part 1. The nature and sources of cloud-active aerosols. *Earth-Science Reviews*, *89*(1), 13–41. https://doi.org/10.1016/j.earscirev.2008.03.001

Ardyna, M., Claustre, H., Sallée, J.-B., D'Ovidio, F., Gentili, B., Van Dijken, G., et al. (2017). Delineating environmental control of phytoplankton biomass and phenology in the Southern Ocean. *Geophysical Research Letters*, *44*, 5016–5024. https://doi.org/10.1002/2016GL072428

Arnold, S. R., Spracklen, D. V., Williams, J., Yassaa, N., Sciare, J., Bonsang, B., et al. (2009). Evaluation of the global oceanic isoprene source and its impacts on marine organic carbon aerosol. *Atmospheric Chemistry and Physics*, *9*(4), 1253–1262. https://doi.org/10.5194/acp-9-1253-2009

Bintanja, R., Severijns, C., Haarsma, R., & Hazeleger, W. (2014). The future of Antarctica's surface winds simulated by a high-resolution global climate model: 1. Model description and validation. *Journal of Geophysical Research: Atmospheres*, *119*, 7136–7159. https://doi.org/10.1002/2013JD020847

Bonsang, B., Gros, V., Peeken, I., Yassaa, N., Bluhm, K., Zöllner, E., et al.(2010). Isoprene emission from phytoplankton monocultures: The relationship with chlorophyll-a, cell volume and carbon content. *Environmental Chemistry*, *7*(6), 554–563. https://doi.org/10.1071/EN09156

Bonsang, B., Polle, C., & Lambert, G. (1992). Evidence for marine production of isoprene. *Geophysical Research Letters*, *19*(11), 1129–1132. https://doi.org/10.1029/92GL00083

Booge, D., Marandino, C. A., Schlundt, C., Palmer, P. I., Schlundt, M., Atlas, E. L., et al. (2016). Can simple models predict large-scale surface ocean isoprene concentrations? *Atmospheric Chemistry and Physics*, *16*(18), 11,807–11,821.

Booge, D., Schlundt, C., Bracher, A., Endres, S., Zäncker, B., & Marandino, C. A. (2018). Marine isoprene production and consumption in the mixed layer of the surface ocean—A field study over two oceanic regions. *Biogeosciences (BG)*, *15*, 649–667. https://doi.org/10.5194/bg-15-649-2018

Brüggemann, M., Hayeck, N., & George, C. (2018). Interfacial photochemistry at the ocean surface is a global source of organic vapors and aerosols. *Nature Communications*, *9*(1), 2101. https://doi.org/10.1038/s41467-018-04528-7

Broadgate, W., Liss, P. D., & Penkett, S. A. (1997). Seasonal emissions of isoprene and other reactive hydrocarbon gases from the ocean. *Geophysical Research Letters*, *24*(21), 2675–2678. https://doi.org/10.1029/97GL02736

Broadgate, W. J., Malin, G., Küpper, F. C., Thompson, A., & Liss, P. S. (2004). Isoprene and other non-methane hydrocarbons from seaweeds: A source of reactive hydrocarbons to the atmosphere. *Marine Chemistry*, *88*(1), 61–73. https://doi.org/10.1016/j.marchem.2004.03.002

Carpenter, L. J., Archer, S. D., & Beale, R. (2012). Ocean-atmosphere trace gas exchange. *Chemical Society Reviews*, *41*(19), 6473–6506. https://doi.org/10.1039/C2CS35121H

Carslaw, K. S., Lee, L. A., Reddington, C. L., Pringle, K. J., Rap, A., Forster, P. M., et al. (2013). Large contribution of natural aerosols to uncertainty in indirect forcing. *Nature*, *503*(7474), 67–71. https://doi.org/10.1038/nature12674

Ciuraru, R., Fine, L., van Pinxteren, M., D'Anna, B., Herrmann, H., & George, C. (2015). Photosensitized production of functionalized and unsaturated organic compounds at the air-sea interface. *Scientific Reports*, *5*, 12741. https://doi.org/10.1038/srep12741

Claeys, M., Graham, B., Vas, G., Wang, W., Vermeylen, R., Pashynska, V., et al. (2004). Formation of secondary organic aerosols through photooxidation of isoprene. *Science*, *303*(5661), 1173–1176. https://doi.org/10.1126/science.1092805

Conte, L., Szopa, S., Aumont, Gros, V., & Bopp, L. (2020). Sources and sinks of isoprene in the global open ocean: Simulated patterns and emissions to the atmosphere. *Journal of Geophysical Research: Oceans*, *125*, e2019JC015946. https://doi.org/10.1029/2019JC015946

Dani, KGS, & Loreto, F. (2017). Trade-off between dimethyl sulfide and isoprene emissions from marine phytoplankton. *Trends in Plant Science*, *22*(5), 361–372. https://doi.org/10.1016/j.tplants.2017.01.006

Exton, D. A., Suggett, D. J., McGenity, T. J., & Steinke, M. (2013). Chlorophyll-normalized isoprene production in laboratory cultures of marine microalgae and implications for global models. *Limnology and Oceanography*, *58*(4), 1301–1311. https://doi.org/10.4319/lo.2013.58.4.1301

Fay, A. R., & McKinley, G. A. (2014). Global open-ocean biomes: mean and temporal variability. *Earth System Science Data*, *6*(2), 273–284. https://doi.org/10.5194/essd-6-273-2014

Galí, M., Devred, E., Babin, M., & Levasseur, M. (2019). Decadal increase in Arctic dimethylsulfide emission. *Proceedings of the National Academy of Sciences*, *116*(39), 19,311–19,317. https://doi.org/10.1073/pnas.1904378116

Galí, M., Levasseur, M., Devred, E., Simó, R., & Babin, M. (2018). Sea-surface dimethylsulfide (dms) concentration from satellite data at global and regional scales. *Biogeosciences*, *15*(11), 3497–3519. https://doi.org/10.5194/bg-15-3497-2018

Gantt, B., Meskhidze, N., & Kamykowski, D. (2009). A new physically-based quantification of isoprene and primary organic aerosol emissions from the world's oceans. *Atmospheric Chemistry and Physics*, *9*, 2933–2965. https://doi.org/10.5194/acp-9-4915-2009

Hackenberg, S. C., Andrews, S. J., Airs, R., Arnold, S. R., Bouman, H. A., Brewin, R. J. W., et al. (2017). Potential controls of isoprene in the surface ocean. *Global Biogeochemical Cycles*, *31*, 644–662. https://doi.org/10.1002/2016GB005531

Holte, J., Talley, L. D., Gilson, J., & Roemmich, D. (2017). An argo mixed layer climatology and database. *Geophysical Research Letters*, *44*, 5618–5626. https://doi.org/10.1002/2017GL073426

Kameyama, S., Yoshida, S., Tanimoto, H., Inomata, S., Suzuki, K., & Yoshikawa-Inoue, H. (2014). High-resolution observations of dissolved isoprene in surface seawater in the Southern Ocean during austral summer 2010–2011. *Journal of Oceanography*, *70*(3), 225–239. https://doi.org/10.1007/s10872-014-0226-8

Kim, M. J., Novak, G. A., Zoerb, M. C., Yang, M., Blomquist, B. W., Huebert, B. J., et al. (2017). Air-sea exchange of biogenic volatile organic compounds and the impact on aerosol particle size distributions. *Geophysical Research Letters*, *44*, 3887–3896. https://doi.org/10.1002/2017GL072975

Legendre, P., & Legendre, L. F. J. (2012). *Numerical ecology*, 24, (1–990). Amsterdam, The Netherlands: Elsevier.

Lewis, A. C., Hopkins, J. R., Read, K. A., Carpenter, L. J., Pilling, M. J., & Stanton, J. (2005). Sources and sinks of acetaldehyde, acetone and methanol in North Atlantic marine boundary layer air. *Atmospheric Chemistry and Physics*, *5*, 1963–1974. https://doi.org/10.5194/acp-5-1963-2005

Liakakou, E., Vrekoussis, M., Bonsang, B., Donousis, C., Kanakidou, M., & Mihalopoulos, N. (2007). Isoprene above the eastern Mediterranean: Seasonal variation and contribution to the oxidation capacity of the atmosphere. *Atmospheric Environment*, *41*(5), 1002–1010. https://doi.org/10.1016/j.atmosenv.2006.09.034

Liao, H., Henze, D. K., Seinfeld, J. H., Wu, S., & Mickley, L. J. (2007). Biogenic secondary organic aerosol over the United States: Comparison of climatological simulations with observations. *Journal of Geophysical Research*, *112*, D06201. https://doi.org/10.1029/2006JD007813

Longhurst, A. (1995). Seasonal cycles of pelagic production and consumption. *Progress in oceanography*, *36*(2), 77–167. https://doi.org/10.1016/0079-6611(95)00015-1

Luo, G., & Yu, F. (2010). A numerical evaluation of global oceanic emissions of α-pinene and isoprene. *Atmospheric Chemistry and Physics*, *10*(4), 2007–2015. https://doi.org/10.5194/acp-10-2007-2010

McKay, W. A., Turner, M. F., Jones, B. M. R., & Halliwell, C. M. (1996). Emissions of hydrocarbons from marine phytoplankton—Some results from controlled laboratory experiments. *Atmospheric Environment*, *30*(14), 2583–2593. https://doi.org/10.1016/1352-2310(95)00433-5

Medeiros, D. J., Blitz, M. A., James, L., Speak, T. H., & Seakins, P. W. (2018). Kinetics of the reaction of OH with isoprene over a wide range of temperature and pressure including direct observation of equilibrium with the OH adducts. *The Journal of Physical Chemistry A*, *122*(37), 7239–7255. https://doi.org/10.1021/acs.jpca.8b04829

Meier, W., Fetterer, F., Savoie, M., Mallory, S., Duerr, R., & Stroeve, J. (2017). Noaa/nsidc climate data record of passive microwave sea ice concentration, version 3, National Snow and Ice Data Center. https://doi.org/10.7265/N59P2ZTG

Meskhidze, N., & Nenes, A. (2006). Phytoplankton and cloudiness in the Southern Ocean. *Science*, *314*(5804), 1419–1423. https://doi.org/10.1126/science.1131779

Meskhidze, N., Sabolis, A., Reed, R., & Kamykowski, D. (2015). Quantifying environmental stress-induced emissions of algal isoprene and monoterpenes using laboratory measurements. *Biogeosciences*, *12*(3), 637–651. https://doi.org/10.5194/bgd-11-13533-2014

Milne, Riemer, Zika, & Brand (1995). Measurement of vertical distribution of isoprene in surface seawater, its chemical fate, and its emission from several phytoplankton monocultures. *Marine Chemistry*, *48*(3), 237–244. https://doi.org/10.1016/0304-4203(94)00059-M

Moore, R. M., Oram, D. E., & Penkett, S. A. (1994). Production of isoprene by marine phytoplankton cultures. *Geophysical Research Letters*, *21*(23), 2507–2510. https://doi.org/10.1029/94GL02363

Moutier, W., Thomalla, S. J., Bernard, S., Wind, G., Ryan-Keogh, T. J., & Smith, M. E. (2019). Evaluation of chlorophyll-a and POC MODIS aqua products in the Southern Ocean. *Remote Sensing*, *11*(15), 1793. https://doi.org/10.3390/rs11151793

Mungall, E. L., Abbatt, J. P. D., Wentzell, J. J. B., Lee, A. lexK. Y., Thomas, J. L., Blais, M., et al. (2017). Microlayer source of oxygenated volatile organic compounds in the summertime marine arctic boundary layer. *Proceedings of the National Academy of Sciences*, *114*(24), 6203–6208. https://doi.org/10.3390/rs11151793

Neukermans, G., Harmel, T., Galí, M., Rudorff, N., Chowdhary, J., Dubovik, O., et al. (2018). Harnessing remote sensing to address critical science questions on ocean-atmosphere interactions. *Elementa: Science of the Anthropocene*, *6*(1), 71. https://doi.org/10.1525/elementa.331

Nunes, S., Latasa, M., Delgado, M., Emelianov, M., Simó, R., & Estrada, M. (2019). Phytoplankton community structure in contrasting ecosystems of the Southern Ocean: South Georgia, South Orkneys and Western Antarctic peninsula. *Deep Sea Research Part I: Oceanographic Research Papers*, *151*, 103059. https://doi.org/10.1016/j.dsr.2019.06.005

O'Dowd, C. D., Facchini, M. C., Cavalli, F., Ceburnis, D., Mircea, M., Decesari, S., et al. (2004). Biogenically driven organic contribution to marine aerosol. *Nature*, *431*(7009), 676–680.

Ooki, A., Nomura, D., Nishino, S., Kikuchi, T., & Yokouchi, Y. (2015). A global-scale map of isoprene and volatile organic iodine in surface seawater of the Arctic, Northwest Pacific, Indian, and Southern Oceans. *Journal of Geophysical Research: Oceans*, *120*, 4108–4128. https://doi.org/10.1002/2014JC010519

Palmer, P. I., & Shaw, S. L. (2005). Quantifying global marine isoprene fluxes using modis chlorophyll observations. *Geophysical Research Letters*, *32*, L09805. https://doi.org/10.1029/2005GL022592

Peng, G., Meier, W. N., Scott, D. J., & Savoie, M. H. (2013). A long-term and reproducible passive microwave sea ice concentration data record for climate studies and monitoring. *Earth System Science Data*, *5*, 311–318. https://doi.org/10.5194/essd-5-311-2013

Rodrguez-Ros, P., Corts, P., Robinson, C. M., Hassler, C., Royer, S.-J., Estrada, M., et al. (2020). Distribution and drivers of marine isoprene concentration across the Southern Ocean. *Atmosphere*, *11*, 556. https://doi.org/10.3390/atmos11060556

Shaw, S. L., Chisholm, S. W., & Prinn, R. G. (2003). Isoprene production by prochlorococcus, a marine cyanobacterium, and other phytoplankton. *Marine Chemistry*, *80*(4), 227–245. https://doi.org/10.1016/S0304-4203(02)00101-9

Shaw, S. L., Gantt, B., & Meskhidze, N. (2010). Production and emissions of marine isoprene and monoterpenes: A review. *Advances in Meteorology*, *2010*, 24.

Vallina, S. M., Simó, R., Gassó, S., de Boyer-Montégut, C., Del Río, E., Jurado, E., & Dachs, J.(2007). Analysis of a potential solar radiation dose–dimethylsulfide–cloud condensation nuclei link from globally mapped seasonal correlations. *Global Biogeochemical Cycles*, *21*, GB2004. https://doi.org/10.1029/2006GB002787

Wanninkhof, R. (2014). Relationship between wind speed and gas exchange over the ocean revisited. *Limnology and Oceanography: Methods*, *12*(6), 351–362. https://doi.org/10.4319/lom.2014.12.351

Wingenter, O. W., Haase, K. B., Strutton, P., Friederich, G., Meinardi, S., Blake, D. R., & Rowland, F. S. (2004). Changing concentrations of CO, CH_4, C_5H_8, CH_3Br, CH_3I, and dimethyl sulfide during the Southern Ocean iron enrichment experiments. *Proceedings of the National Academy of Sciences of the United States of America*, *101*(23), 8537–8541. https://doi.org/10.1073/pnas.0402744101

Wohl, C., Brown, I., Kitidis, V., Jones, A. E., Sturges, W. T., Nightingale, P. D., & Yang, M. (2020). Underway seawater and atmospheric measurements of volatile organic compounds in the Southern Ocean. *Biogeosciences Discussions*, *2020*, 1–40. https://doi.org/10.5194/bg-2020-2

Zamanillo, M., Ortega-Retuerta, E., Nunes, S., Estrada, M., Sala, M. M., Royer, S.-J., et al. (2019). Distribution of transparent exopolymer particles (TEP) in distinct regions of the Southern Ocean. *Science of The Total Environment*, *691*, 736–748. https://doi.org/10.1016/j.marchem.2009.06.004

Zindler, C., Marandino, C. A., Bange, H. W., Schütte, F., & Saltzman, E. S. (2014). Nutrient availability determines dimethyl sulfide and isoprene distribution in the Eastern Atlantic Ocean. *Geophysical Research Letters*, *41*, 3181–3188. https://doi.org/10.1002/2014GL059547